Integrating Energy Storage Systems – Optimal Power Flow Problem

Project Report

Mats Kraft

7370653

Model evaluation & interpretation

Rolf Schnaufer

7409069

Introduction & weather scenario simulation

Niklas Droßmann

7419092

Optimization model design

Lecturer: Dr. Saber Talari

Teaching Assistant: Lennard Sund

University of Cologne

Department of Information Systems for Sustainable Society

Cologne, February 28th, 2025

Abstract

In this study we examine the integration of an Energy Storage System (EES) with non-simultaneous charging and discharging into an electricity system with high reliance on renewable energy sources. The implemented EES is largely based on previous work of Garifi et al. (2020). We generate three scenarios for wind and solar energy using Monte Carlo simulation from historical data of the wind farm Klim in Denmark as well as Renewables.ninja. We formulate and deploy two optimization problems in Julia to assess the impact of EES integration for all scenarios independently and scale renewable generation output accordingly and deterministically. Our results showcase that the integration of EES significantly improves system reliability and increases social welfare in all examined cases. We emphasize the need for energy storage integration in systems where reliance on renewable energy sources is high, for example when capacity of traditional generators or transmission lines is limited. In these cases, EES can play a significant role in preventing load shortages.

Contents

List of Figures

1 Introduction

The increasing integration of renewable energy sources into modern power systems introduces complex challenges due to their inherent variability and stochastic nature (Morales et al., 2014). Wind and solar power, the most prevalent renewable sources, exhibit fluctuations that complicate grid stability and market efficiency (Conejo et al., 2016). To address these challenges, Energy Storage Systems (ESS) offer a promising solution by providing flexible load balancing, mitigating price volatility, and improving overall system reliability (Kazempour et al., 2016). However, integrating ESS into power markets necessitates advanced optimization techniques to ensure their economic viability and technical effectiveness (Morales et al., 2014).

Recent studies highlight that ESS enhance energy reliability, facilitate demand flexibility, and improve power system resilience (Sousa, Lagarto, & Barata, 2025). Grid-scale applications, such as pumped hydro and battery storage, are particularly effective in mitigating renewable uncertainty while optimizing dispatchable generation (Čičić et al., 2025). On a smaller scale, home energy management systems (HEMS) demonstrate how predictive control algorithms optimize ESS operation with solar photovoltaics (PV), improving selfconsumption and efficiency under dynamic electricity pricing (Garifi et al., 2018). However, challenges remain in coordinating ESS operation, particularly in avoiding simultaneous charging and discharging. Our work builds upon these insights by integrating stochastic renewable generation modelling with deterministic optimization, assessing the impact of ESS on market efficiency and system reliability.

To model renewable generation variability, we employ Monte Carlo simulations to generate wind and solar energy scenarios, a common approach in stochastic optimization (Baringo & Conejo, 2013). Wind data distributions are derived from historical datasets associated with the Klim wind farm (Pinson, 2013), while solar generation profiles are sourced from Renewables.Ninja for the same location (Pfenninger & Staffell, 2016). The study defines three distinct weather scenarios: Stormy (high wind, low solar), Blue Sky (low wind, high solar), and Cloudy (moderate wind, low solar), ensuring a comprehensive evaluation of system behaviour under different conditions.

The optimization framework employed in this study operates over a 42-hour horizon and follows a social welfare maximization approach. The model incorporates constraints on transmission line capacities, generator dispatch limits, and energy storage operations, enforcing non-simultaneous charging and discharging constraints. By comparing cases with and without ESS, we quantify its influence on market efficiency and overall economic performance (Conejo et al., 2016).

The remainder of this report is structured as follows. The methodology section outlines the scenario generation process, optimization model formulation, and ESS role in market clearing. The results section presents comparative analyses across different scenarios, highlighting the contributions of ESS to system stability and economic welfare. In the Discussion, we interpret the findings in the broader context of electricity market operations, while summarizing key insights and potential avenues for future research.

2 Methodology

This section details the methodological framework used to assess the impact of ESS in a 4-bus test case under varying weather conditions. First, we describe the weather scenario simulation, where wind and solar generation profiles are generated using Monte Carlo simulations based on historical data from the Klim wind farm in Denmark and Renewables.ninja. Next, the design of the optimization model is outlined, incorporating power flow constraints, generator dispatch, and ESS dynamics within a social welfare maximization framework. Finally, the integration of an energy storage system is discussed, highlighting the role of ESS in improving system stability and economic efficiency by enforcing non-simultaneous charging and discharging constraints. The methodology ensures a realistic assessment of how storage deployment enhances market performance across different renewable generation scenarios.

2.1 Weather scenario simulation

To evaluate the impact of ESS in a realistic power system setting, we generated stochastic weather scenarios for wind and solar energy using Monte Carlo simulations. Monte Carlo simulations are often applied in renewable energy forecasting to account for the stochastic nature of wind and solar power generation. Prior studies have demonstrated that these methods effectively capture the variability of renewable energy sources, enabling more accurate system planning and operational strategies (Twaróg, 2025; Sircar, Shrivats, & Yang, 2024). Monte Carlo-based stochastic modelling has been applied to assess climate variability impacts on hybrid power systems, helping to optimize the share of wind and solar generation (Twaróg, 2025). Our study adopts a similar approach by introducing controlled randomness to historical datasets, ensuring representative energy scenarios. The primary goal was to create representative time series that capture the inherent variability of renewable generation while ensuring a structured approach to scenario selection. For wind energy, we used historical wind power data from the Klim wind farm in Denmark (Bukhsh et al., 2016; Pinson, 2013). The simulation process followed these steps:

1. *Scenario Selection:* Based on our tutor's guidance, we chose one representative wind zone and generated three distinct Monte Carlo scenarios by introducing controlled randomness into the original dataset.
2. *Hourly Averaging:* Each Monte Carlo run produced multiple realizations of wind generation over the 42-hour timeframe. The final values for each scenario were obtained by calculating the hourly mean across simulations.
3. *Deterministic Storage:* These averaged values were stored in a structured data format to serve as fixed inputs for the optimization model, ensuring that the stochastic component was integrated but deterministic values were used for optimization.

We decided to simulate three distinct weather scenarios to model renewable energy variability, capturing fluctuations in both wind and solar power. Due to the different statistical properties of these energy sources, our approach required specific adjustments:

1. Wind Power Modelling: Variability was introduced by applying stochastic perturbations to historical wind data, ensuring representative time series that reflect real-world fluctuations.

2. Solar Power Adjustments: Unlike wind, solar follows a predictable diurnal pattern, peaking at midday and dropping overnight. To maintain realism, bounded Monte Carlo perturbations were applied to account for cloud coverage and irradiance variation.

Regarding meteorological consistency, wind and solar scenarios were logically paired, rather than combined randomly. Previous research has emphasized the importance of scenario matching, as uncorrelated selections can lead to unrealistic results (Rajendrane, Yogarathnam, & Zhao, 2024). Based on real-world weather patterns (Xu, Zhou, & Zhang, 2024), we established the following structured relationships:

- **Stormy** conditions: High wind availability paired with low solar generation.

- **Blue sky** conditions: Low wind speeds, requiring greater reliance on conventional generation, paired with high solar output under clear skies.

- **Cloudy** conditions: Moderate wind and solar availability, reflecting balanced weather patterns.

The Monte Carlo-generated outputs were stored in a deterministic format, balancing stochastic variability with computational efficiency. This approach aligns with prior studies in renewable energy forecasting, where deterministic optimization models assess the economic and operational impacts of renewable fluctuations (Moradi, Tanneau, & Zandehshahvar, 2025). By applying stochastic modelling at the scenario generation stage, while keeping the optimization framework deterministic, we enhance both realism and computational feasibility.

2.2 Design of the optimization model

This section will focus on the design of the optimization model. We present the model environment and lay down the mathematical foundation.

2.2.1 Model environment

The optimization model was built around a simulated energy system environment consisting of four busses, as illustrated in Figure 1. The system contains two places where energy is demanded - bus 3 and 4, with a load of 70 MW and 40 MW, respectively. Three sources of energy are simulated: a conventional steam turbine generator at bus 1 with a capacity of 90 MW, a wind farm at bus 2 with a capacity of 60 MW and a solar park at bus 4 with a capacity of 60 MW. As the generated wind and solar scenarios values act as scalars ranging from 0 to 1, the energy output from the renewables were scaled accordingly to their scenarios for each time step. Busses are connected through transmission lines, with lines 1, 2 and 3 being limited by a capacity of 50 MW, 100 MW and 80 MW, respectively.

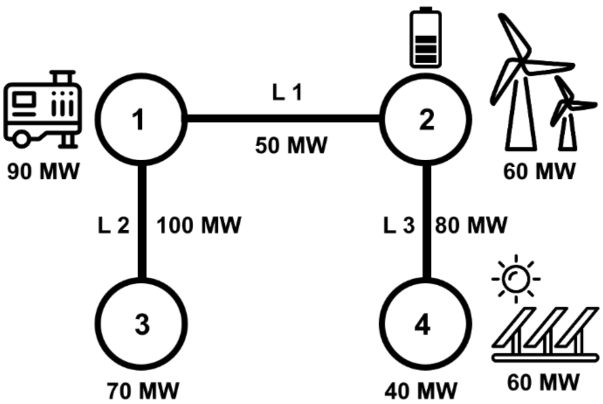

Figure 1. Model environment overview

The operators of the steam turbine generator at bus 1 offer their electricity for a price of 12€/MWh, with bus 3 and 4 submitting their bids as 40€/MWh and 35€/MWh. The performance evaluation of the ESS requires a comparison of two models, one with the ESS integrated and one without. The model without the ESS will be referred to as model 1, while the ESS model will be referred to as model 2. For model 2, bus 2 is additionally equipped with a battery, as seen in Figure 1.

2.2.2 Mathematical formulation

As model 1 acts as the benchmark without an integrated energy storage, it can be formulated as a conventional optimization problem.

$$max_{D1,D2,G1}\, SW = \sum_{t=1}^{42}\left(40pd_{D1,t} + 35pd_{D2,t} - 12pg_{G1,t}\right) \tag{1a}$$

s.t.

$$0 \leq pg_{G1,t} \leq\ 90 \quad t \in \{1, \ldots ,42\} \tag{1b}$$

$$0 \leq pg_{G2,t} \leq\ 60 \quad t \in \{1, \ldots ,42\} \tag{1c}$$

$$0 \leq pg_{G3,t} \leq\ 90 \quad t \in \{1, \ldots ,42\} \tag{1d}$$

$$-50 \leq 500\left(\delta_{B1,t} - \delta_{B2,t}\right) \leq 50 \ \ t \in \{1, \ldots ,42\} \tag{1e}$$

$$-100 \leq 500\left(\delta_{B1,t} - \delta_{B3,t}\right) \leq 100 \ \ t \in \{1, \ldots ,42\} \tag{1f}$$

$$-80 \leq 500\left(\delta_{B2,t} - \delta_{B4,t}\right) \leq 80 \ \ t \in \{1, \ldots ,42\} \tag{1g}$$

$$pg_{G1,t} - 500\left(\delta_{B1,t} - \delta_{B2,t}\right) - 500\left(\delta_{B1,t} - \delta_{B3,t}\right) = 0 \ : \lambda_{B1} \ \ t \in \{1, \ldots ,42\} \tag{1h}$$

$$pg_{G2,t} - 500\left(\delta_{B1,t} - \delta_{B2,t}\right) - 500\left(\delta_{B2,t} - \delta_{B4,t}\right) = 0 \ : \lambda_{B2} \ \ t \in \{1, \ldots ,42\} \tag{1i}$$

$$-pd_{D1,t} - 500\left(\delta_{B1,t} - \delta_{B3,t}\right) = 0 \ : \lambda_{B3} \ \ t \in \{1, \ldots ,42\} \tag{1j}$$

$$-pd_{D2,t} + pg_{G3,t} - 500\left(\delta_{B2,t} - \delta_{B4,t}\right) = 0 \ : \lambda_{B4} \ \ t \in \{1, \ldots ,42\} \tag{1k}$$

$$pg_{G2,t} = wind\_scenario_t \cdot pg_{G2,t} \quad t \in \{1, \ldots ,42\} \tag{1l}$$

$$pg_{G3,t} = solar\_scenario_t \cdot pg_{G3,t} \quad t \in \{1, \ldots ,42\} \tag{1m}$$

$$\delta_{B1,t} =\ 0 \quad t \in \{1, \ldots ,42\} \tag{1n}$$

For model 2, the energy storage system was integrated in form of additional constraints and a modified power equation for bus 2, which were modelled after the approach proposed by Garifi et al. (2018), guaranteeing non-simultaneous charging and discharging. The terms b_dis and b_ch simulate battery discharge and battery charge, while b_soc denotes the battery state of charge. The battery charging and discharging efficiency is implemented through η_c and η_d, standing at 95% and 90%, respectively. Finally, we assume the battery starts at 15 MW in t=1, which equals 30% of its maximum capacity.

$$max_{D1,D2,G1}\, SW = \sum_{t=1}^{42} \left(40pd_{D1,t} + 35pd_{D2,t} - 12pg_{G1,t}\right) \tag{2a}$$

s.t.

$$0 \le pg_{G1,t} \le\ 90 \quad t \in \{1, \dots, 42\} \tag{2b}$$

$$0 \le pg_{G2,t} \le\ 60 \quad t \in \{1, \dots, 42\} \tag{2c}$$

$$0 \le pg_{G3,t} \le\ 90 \quad t \in \{1, \dots, 42\} \tag{2d}$$

$$-50 \le 500\left(\delta_{B1,t} - \delta_{B2,t}\right) \le 50 \ \ t \in \{1, \dots, 42\} \tag{2e}$$

$$-100 \le 500\left(\delta_{B1,t} - \delta_{B3,t}\right) \le 100 \ \ t \in \{1, \dots, 42\} \tag{2f}$$

$$-80 \le 500\left(\delta_{B2,t} - \delta_{B4,t}\right) \le 80 \ \ t \in \{1, \dots, 42\} \tag{2g}$$

$$pg_{G1,t} - 500\left(\delta_{B1,t} - \delta_{B2,t}\right) - 500\left(\delta_{B1,t} - \delta_{B3,t}\right) = 0 \ : \lambda_{B1} \ \ t \in \{1, \dots, 42\} \tag{2h}$$

$$pg_{G2,t} + b_{dis_t} - b_{ch_t} - 500\left(\delta_{B1,t} - \delta_{B2,t}\right) - 500\left(\delta_{B2,t} - \delta_{B4,t}\right) = 0 \ : \lambda_{B2} \quad t \in \{1, \dots, 42\} \tag{2i}$$

$$-pd_{D1,t} - 500\left(\delta_{B1,t} - \delta_{B3,t}\right) = 0 \ : \lambda_{B3} \ \ t \in \{1, \dots, 42\} \tag{2j}$$

$$-pd_{D2,t} + pg_{G3,t} - 500\left(\delta_{B2,t} - \delta_{B4,t}\right) = 0 \ : \lambda_{B4} \ \ t \in \{1, \dots, 42\} \tag{2k}$$

$$pg_{G2,t} = wind\_scenario_t \cdot pg_{G2,t} \quad t \in \{1, \dots, 42\} \tag{2l}$$

$$pg_{G3,t} = solar\_scenario_t \cdot pg_{G3,t} \quad t \in \{1, \dots, 42\} \tag{2m}$$

$$\delta_{B1,t} =\ 0 \quad t \in \{1, \dots, 42\} \tag{2n}$$

$$0 \le b\_soc_t \le 50 \quad t \in \{1, \dots, 42\} \tag{2o}$$

$$0 \le b\_dis_t \le 20 \quad t \in \{1, \dots, 42\} \tag{2p}$$

$$0 \le b\_ch_t \le 20 \quad t \in \{1, \dots, 42\} \tag{2q}$$

$$b\_soc_{t=1} =\ 15 \tag{2r}$$

$$b_{soc_{t+1}} = b_{soc_t} + \eta_c \Delta t\, b_{ch_t} y_t - \eta_d \Delta t\, b_{dis_t}(1 - y_t) \quad t \in \{1, \dots, 42\} \tag{2s}$$

$$y \in \{0,1\}$$

Lastly, the optimization model was solved using the HiGHS solver in Julia. To accurately evaluate the performance of the ESS, both models were run separately for each scenario, resulting in six different outcomes to be presented in the following section.

3 Results

All six optimization scenarios compiled successfully and executed efficiently. The HiGHS solver demonstrated excellent computational performance with a runtime of less than 0.1 seconds for each scenario.

To ensure reproducibility and transparency, the full codebase, weather data files, and optimization model are available in a public repository [https://github.com/matskraft/AMO_GroupProject_SchnauferDrossmannKraft.git]. This allows for further validation and potential extensions of the study.

The following subsections present a comparative analysis of system performance across different scenarios. The results focus on social welfare, generator dispatch, and the impact of ESS on system stability and market efficiency. Next the results of the three weather scenarios over the 42-hour time period will be presented in a subsection each.

3.1 Stormy weather scenario

The total social welfare in the stormy scenario was 137.870,48€ without ESS and 141.569,68€ with ESS, representing a 2.68% increase when storage was included. The results for the case without ESS are illustrated in Figure 2, while the corresponding results with ESS are shown in Figure 3.

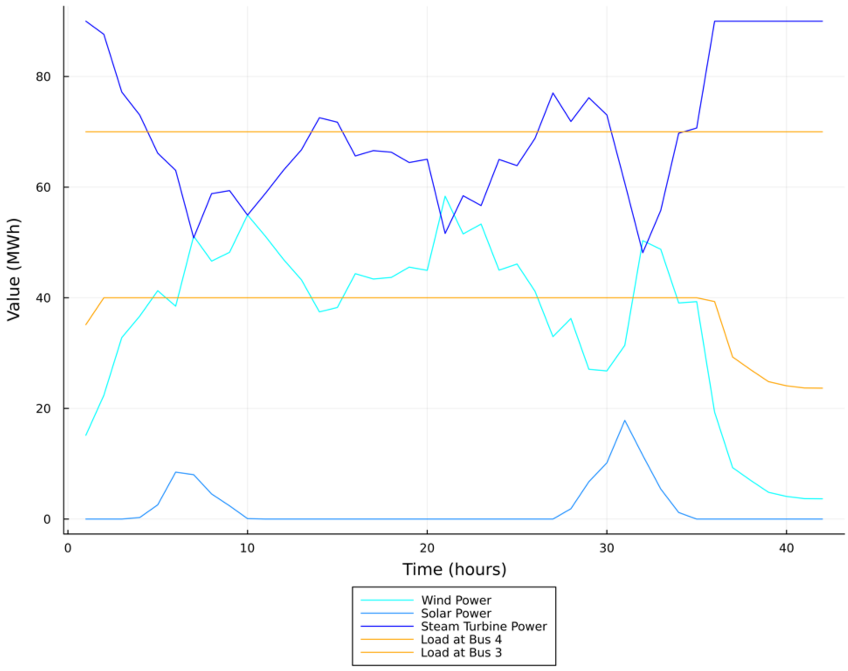

Figure 2. Stormy scenario without ESS

Without ESS, the available generation was insufficient to meet demand at all times, leading to periods where the load at bus 4 could not be fully supplied, particularly at the beginning and end of the time window. During the central hours of the simulation, wind generation was high, allowing both loads to be served completely. However, towards the end of the period, as renewable generation declined, the system was forced to rely on the steam turbine, which operated at maximum capacity. The load at bus 3 was fully met throughout the whole period.

With ESS integration, the results showed a notable improvement in supply reliability. The presence of storage ensured that both loads were continuously served throughout the entire simulation, eliminating the supply shortages observed in the non-ESS case. The storage system, however, remained largely inactive for most of the time, indicating that it was not needed when wind generation was sufficiently high to cover demand. It only became relevant towards the

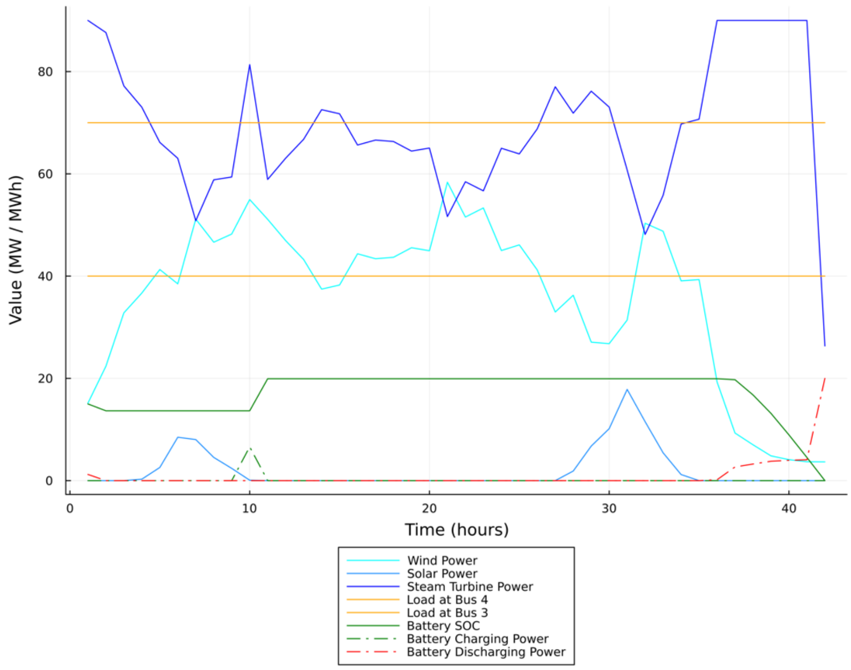

Figure 3. Stormy scenario with ESS

end of the period, when renewable generation declined. At that point, the ESS discharged fully, allowing demand to be met with less in-time generated conventional energy. As a result, the steam turbine, which had been running at full capacity in the non-ESS case, reduced its generation and the remaining demand was covered by the stored energy.

Overall, the results demonstrate that while the ESS was not frequently utilized, its strategic use during critical periods helped to ensure full load coverage and increased overall system welfare. By storing excess power when available and discharging it when renewable generation dropped, the system was able to fully meet the demand.

3.2 Blue sky scenario

The total social welfare in the blue sky scenario was 126.348,18€ without ESS and 132.186,83€ with ESS, corresponding to a 4.62% increase when storage was incorporated. The results for the case without ESS are illustrated in Figure 4, while the corresponding results with ESS are shown in Figure 5.

Without ESS, the system was unable to fully supply the load at bus 4 at multiple points throughout the period. Significant deficits occurred at the beginning and end of the time window, with additional smaller shortfalls scattered throughout the timeframe. In contrast, the load at bus 3 was fully supplied at all times. Throughout the period, the steam turbine played a crucial role in maintaining supply, particularly during hours of lower renewable generation. Towards the end of the time window, as renewable generation decreased, the turbine had to operate at full capacity to compensate for the missing energy, yet this was still insufficient to

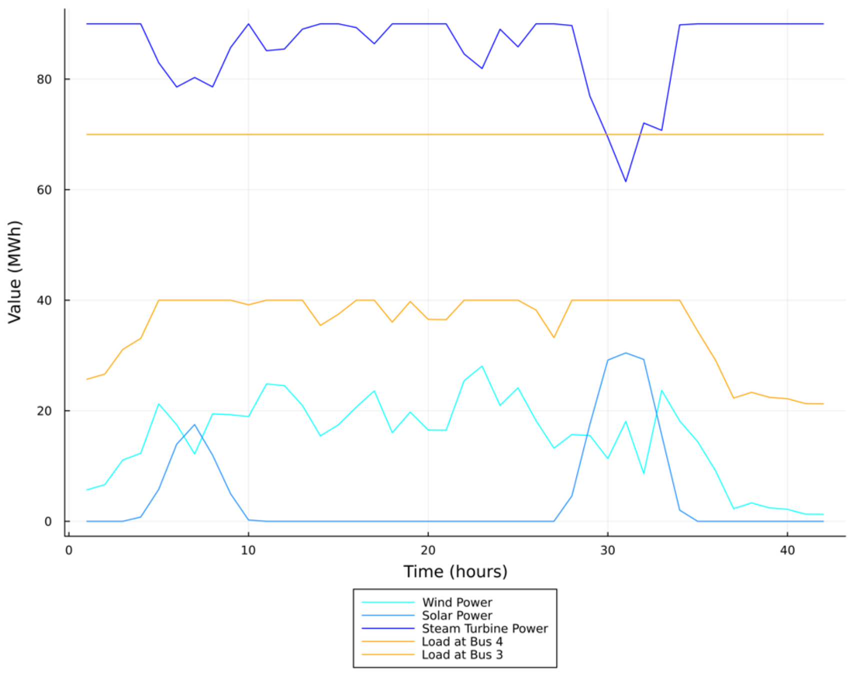

Figure 4. Blue sky scenario without ESS

fully meet demand. Figure 4 highlights these limitations, particularly the recurrent curtailment at bus 4 and the turbine’s maximum output towards the end of the period.

With ESS, the results showed a significant improvement in system reliability, as both loads were fully supplied throughout the entire time window. The steam turbine was observed to operate at full capacity for a longer duration compared to the non-ESS case, indicating that it was also used to charge the battery. Unlike in the stormy scenario, the ESS was frequently in use and switched often between charging and discharging operations, highlighting its dynamic role in balancing supply and demand. Towards the end of the period, when renewable generation declined, the turbine's output was reduced instead of increased, as stored energy was discharged to compensate for the shortfall. This led to a complete depletion of the battery by the end of the simulation. The behaviour of the ESS is clearly depicted in Figure 5, where the state of charge (SOC) follows the curves of the renewable generators with a short delay. Periods of increasing renewable energy are shortly followed by an increase in battery SOC, while decreases in renewable generation lead to a subsequent drop in SOC as stored energy is utilized.

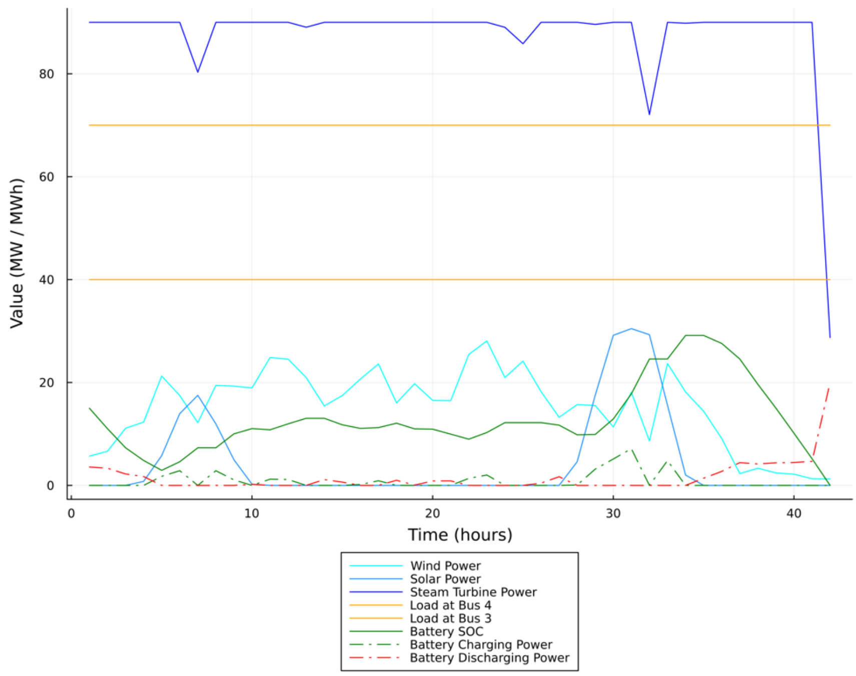

Figure 5. Blue sky scenario with ESS

Overall, the results demonstrate the ability of the ESS to effectively manage fluctuations in renewable generation in this scenario by continuously charging and discharging in response to changing conditions.

3.3 Cloudy scenario

The total social welfare in the cloudy scenario was €129,999.36 without ESS and €134,445.14 with ESS, reflecting a 3.42% increase when storage was included. The results for the case without ESS are illustrated in Figure 6, while the corresponding results with ESS are shown in Figure 7.

Without ESS, the system was unable to fully supply the load at bus 4 at both the beginning and end of the time window, whereas the load at bus 3 was consistently covered. The steam turbine operated at a high capacity throughout the entire period, rarely dropping below 70 MW, as it played a crucial role in balancing demand and renewable fluctuations. The results of this scenario, shown in Figure 6, highlight the limitations of the system, particularly in its inability to fully serve all demand at all times despite the continuous use of conventional generation.

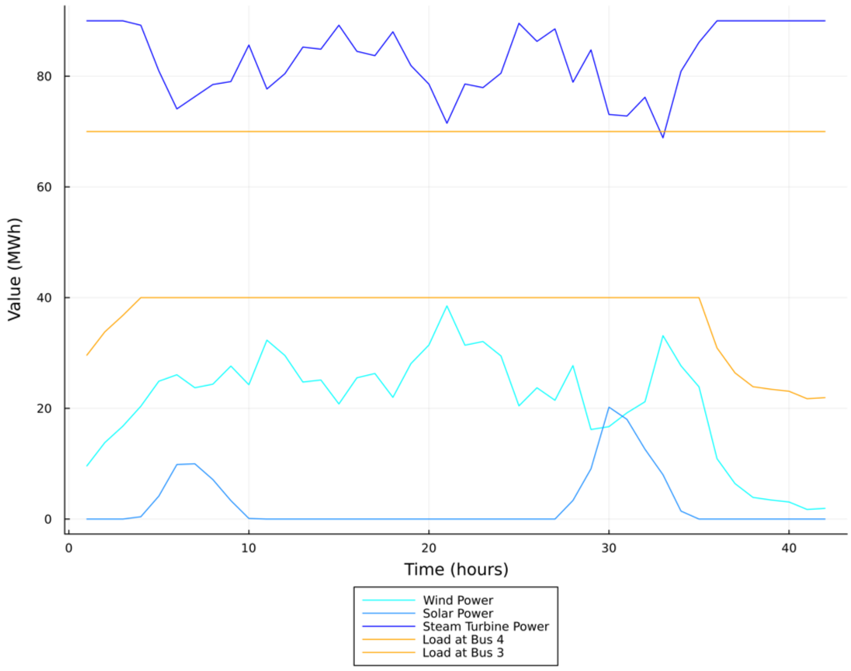

Figure 6. Cloudy scenario without ESS

With ESS, the supply reliability improved, as both loads were fully served throughout the entire simulation. The steam turbine exhibited a different generation pattern, showing even more fluctuations compared to the case without ESS. The battery was actively used, undergoing multiple charging and discharging cycles throughout the period. Unlike in the previous scenarios, the ESS exhibited a clear upward trend in its state of charge (SOC) during the middle hours, following an initial discharge phase at the beginning of the time window to compensate for the missing energy. Towards the end of the period, the battery was fully depleted, supplying the remaining load and allowing the steam turbine output to be reduced accordingly. These dynamics are depicted in Figure 7, where the SOC curve shows a continuous increase before dropping sharply towards the end, mirroring changes in renewable generation and load demand.

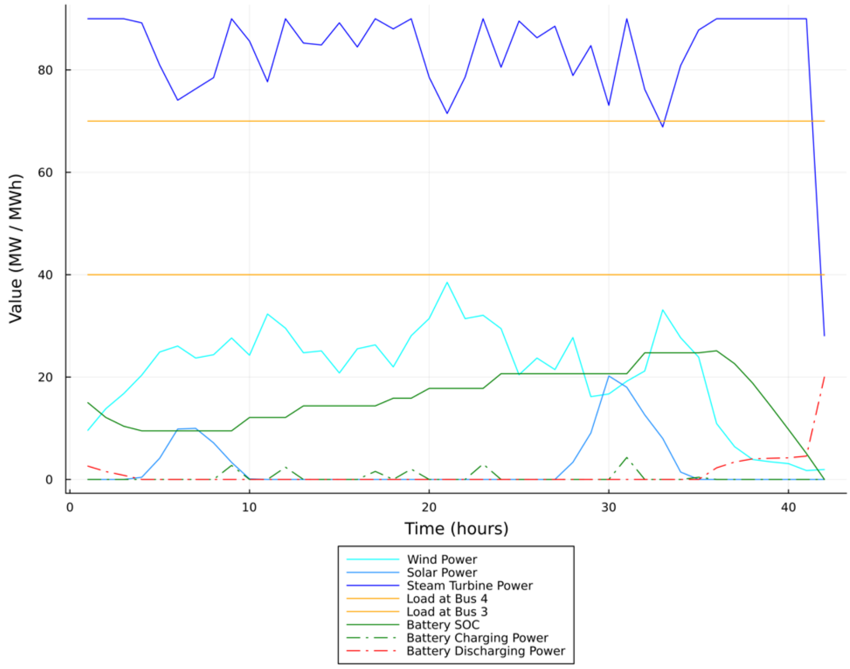

Figure 7. Cloudy scenario with ESS

Overall, the results demonstrate the active role of the ESS in balancing energy fluctuations, particularly in a scenario where neither wind nor solar generation is dominant.

4 Discussion

The results of the optimization study provide valuable insights into the role of ESS in managing renewable energy variability and improving system efficiency. Across all three weather scenarios — stormy, blue sky, and cloudy — integrating ESS consistently increased social welfare and ensured full load coverage. However, the way in which ESS contributed to system stability varied depending on the characteristics of each scenario.

4.1 Common patterns and differences across scenarios

A consistent trend observed in all three scenarios was that ESS eliminated unserved load at bus 4, which otherwise experienced shortages, particularly at the beginning and end of the time window. This highlights the ability of storage to buffer supply shortages, ensuring demand fulfilment even when renewable generation was insufficient. Notably, without ESS, the bus closest to the renewable sources was the one experiencing shortages, reinforcing the expectation that renewable energy sources introduce uncertainty and potential unreliability due to their variability. With ESS, these supply gaps were effectively mitigated, enhancing overall system stability.

The extent of battery utilization varied depending on the available renewable energy supply. In scenarios with high renewable generation, the battery was rarely used, while in scenarios with lower renewable availability, it became increasingly important. In some cases, when renewable generation was insufficient overall, the steam turbine was used to charge the battery, ensuring that stored energy could later be dispatched to fulfil demand. This behaviour reflects the overarching goal of the system optimization — to meet the load demand in the most efficient way possible.

These findings support the broader argument that ESS enhances system flexibility and reliability, aligning with existing literature emphasizing storage as a key enabler of renewable integration (Denholm et al., 2011; Budischak et al., 2013). Previous research has highlighted that ESS reduces unserved demand and minimizes reliance on conventional generation, which is consistent with the observed reduction in load curtailment and improved dispatch patterns in this study.

4.2 Limitations and future research

While the study provides valuable insights, several limitations should be acknowledged. First, the ESS was initialized at 30% state of charge (SOC) and allowed to fully discharge by the end of the timeframe, which does not reflect a real-world scenario where storage systems typically maintain operational reserves. Future work could introduce a constraint requiring the ESS to retain a minimum SOC at the end of the optimization period to better reflect practical use cases.

Additionally, the optimization model assumes perfect foresight, meaning it operates with full knowledge of upcoming fluctuations in renewable generation. In reality, grid operators rely on weather forecasts, which introduce uncertainty. A more realistic approach would be to integrate forecast errors or probabilistic optimization methods to reflect real-world decision-making challenges. The weather scenarios were pre-defined in a stochastic manner rather than modelled as a fully stochastic optimization problem. While this simplifies computational complexity, it reduces realism. Future studies could explore fully stochastic approaches to assess the robustness of storage strategies under greater uncertainty.

Another limitation is the small case study size, consisting of only four buses, three generators, three transmission lines, and two loads. While this provides a controlled environment for analysis, real-world systems are far more complex. Expanding the model to a larger-scale network with more diverse generation and load profiles would provide deeper insights.

Finally, the study considered only a single ESS located at one bus. In real power systems, multiple distributed storage systems interact, and transmission constraints often limit power flow between buses. Investigating how multiple ESS units affect system efficiency, particularly in transmission-constrained networks, would be an important avenue for further research.

5 Conclusion

In summary, the study demonstrates that ESS plays a crucial role in mitigating supply shortages, improving load fulfilment, and increasing social welfare. However, the extent of storage utilization depends on the availability of renewable generation, with lower renewable output leading to greater reliance on storage. While the model provides strong evidence for the benefits of ESS, further research is needed to address real-world uncertainties, expand system complexity, and explore distributed storage solutions in constrained networks.

Bibliography

[1] Pfenninger, Stefan and Staffell, Iain (2016). Long-term patterns of European PV output using 30 years of validated hourly reanalysis and satellite data. Energy 114, pp. 1251-1265. doi: 10.1016/j.energy.2016.08.060

[2] Staffell, Iain and Pfenninger, Stefan (2016). Using Bias-Corrected Reanalysis to Simulate Current and Future Wind Power Output. Energy 114, pp. 1224-1239. doi: 10.1016/j.energy.2016.08.068

[3] Baringo, L., & Conejo, A. J. (2013, pp. 45-52). *Stochastic Programming Approaches for Power System Planning Under Uncertainty*. Springer.

[4] Conejo, A. J., Baringo, L., Kazempour, S. J., & Siddiqui, A. S. (2016, pp. 120-135). *Investment in Electricity Generation and Transmission: Decision Making under Uncertainty*. Springer.

[5] Kazempour, S. J., Conejo, A. J., & Sioshansi, R. (2016). *Market Operations in Electric Power Systems: Forecasting, Scheduling, and Risk Management*. Cambridge University Press.

[6] Morales, J. M., Conejo, A. J., Madsen, H., Pinson, P., & Zugno, M. (2014, pp. 88-97). *Integrating Renewables in Electricity Markets: Operational Problems*. Springer.

[7] Pinson, P. (2013, pp. 564-585). *Wind Energy: Forecasting Challenges for its Operational Management*. Statistical Science, 28(4)

[8] Bukhsh, W. A., Zhang, C., & Pinson, P. (2016). An integrated multiperiod OPF model with demand response and renewable generation uncertainty. *IEEE Transactions on Smart Grid, 7*(3), pp. 1495–1503. https://doi.org/10.1109/TSG.2015.2502723

[9] Denholm, P, Ela, E, Kirby, B, & Milligan, M (2010). Role of Energy Storage with Renewable Electricity Generation. https://doi.org/10.2172/972169

[10] Budischak, C., Sewell, D., Thomson, H., Mach, L., Veron, D. E., & Kempton, W. (2013). Cost-minimized combinations of wind power, solar power and electrochemical storage, powering the grid up to 99.9% of the time. journal of power sources, 225, 60-74

[11] Twaróg, B. S. (2025). *Change in optimal shares of PV and wind in hybrid power plants in Europe due to climate variability using the Monte Carlo method*. Preprints.org. Retrieved from https://www.preprints.org/frontend/manuscript/cb78c2290dc0a9a7209965a125bd4e97/download_pub

[12] Sircar, R., Shrivats, A., & Yang, X. (2024). *Quantifying renewables reliability risk in modern and future electricity grids*. *SSRN Papers*. Retrieved from https://papers.ssrn.com/sol3/Delivery.cfm?abstractid=4917976

[13] Rajendrane, S., Yogarathnam, A., & Zhao, T. (2024). *Diversifying transmission planning of wind-heavy systems by incorporating dynamic line rating*. IEEE Xplore. Retrieved from https://ieeexplore.ieee.org/abstract/document/10741620/

[14] Xu, W., Zhou, X., & Zhang, T. (2024). *Reliability assessment of islanded microgrids considering generation-load uncertainty*. *China Automation Congress*. Retrieved from https://ieeexplore.ieee.org/abstract/document/10865653/

[15] Moradi, A., Tanneau, M., & Zandehshahvar, R. (2025). *Enhanced renewable energy forecasting and operations through probabilistic forecast aggregation*. arXiv Preprint. Retrieved from https://arxiv.org/pdf/2502.07010

[16] Sousa, J., Lagarto, J., & Barata, F. (2025). *Demand flexibility on renewable energy integration, backup capacity, storage use and dispatchable generation: A case study for Portugal's 2030 national energy strategy.* Energy. Retrieved from https://www.sciencedirect.com/science/article/abs/pii/S0360544225009120

[17] Čičić, M., Vivas, C., Canudas-de-Wit, C., & Almeida, L. (2025). *Active network management via grid-friendly electromobility control for curtailment minimization.* Control Engineering Practice. Retrieved from https://www.sciencedirect.com/science/article/pii/S0967066125000528

[18] Garifi, M., Piegari, L., & Rizzo, R. (2018). *Home energy management system with renewable energy integration: A model predictive control approach.* IEEE Transactions on Smart Grid, 9(3), 2070-2081. https://doi.org/10.1109/TSG.2017.2726940

Eidesstattliche Versicherung

Hiermit versichere ich an Eides statt, dass ich die vorliegende Arbeit selbstständig und ohne die Benutzung anderer als der angegebenen Hilfsmittel angefertigt habe. Alle Stellen, die wörtlich oder sinngemäß aus veröffentlichten und nicht veröffentlichten Schriften entnommen wurden, sind als solche kenntlich gemacht. Die Arbeit ist in gleicher oder ähnlicher Form oder auszugsweise im Rahmen einer anderen Prüfung noch nicht vorgelegt worden. Ich versichere, dass die eingereichte elektronische Fassung der eingereichten Druckfassung vollständig entspricht.

Die Strafbarkeit einer falschen eidesstattlichen Versicherung ist mir bekannt, namentlich die Strafandrohung gemäß § 156 StGB bis zu drei Jahren Freiheitsstrafe oder Geldstrafe bei vorsätzlicher Begehung der Tat bzw. gemäß § 161 Abs. 1 StGB bis zu einem Jahr Freiheitsstrafe oder Geldstrafe bei fahrlässiger Begehung.

Niklas Droßmann

Rolf Schnaufer

Mats Kraft